energy&fuels

Article

pubs.acs.org/EF

Revisiting Asphaltene Deposition Tool (ADEPT): Field Application

Anjushri S. Kurup,*[,†] Jianxin Wang,[‡] Hariprasad J. Subramani,[‡] Jill Buckley,[§] Jefferson L. Creek,[‡] and Walter G. Chapman[†]

[†]Department of Chemical and Biomolecular Engineering, Rice University, Houston, Texas 77251, United States

[‡]Chevron Energy Technology Company, Houston, Texas 77002, United States

[§]Petroluem Recovery Research Center, New Mexico Institute of Mining and Technology, Socorro, New Mexico 87801, United States

ABSTRACT: Asphaltenes tend to deposit in reservoir, well tubing, flow lines, separators, etc., causing significant production losses. Asphaltenes are originally stable in crude oil at reservoir conditions. However, changes in temperature, pressure, and/or composition may cause asphaltenes to precipitate and potentially deposit onto the surfaces of a flowing conduit. There are several publications in the literature that discuss modeling of asphaltene phase behavior in oil as well as development of deposition models to simulate asphaltene deposition profiles along a flow path. In this paper, a previously reported asphaltene deposition tool (ADEPT) is used to study the deposition in a subsea pipeline in the Gulf of Mexico. This is the first demonstration of an asphaltene deposition simulator that has been used in a fully predictive manner. All of the required kinetic parameters used for deposition predictions were experimentally measured. A new methodology to scale up the deposition constant measured from a small-scale capillary deposition experiment to a large-scale subsea flow line is also reported in this paper. The predictions that made use of such an appropriately scaled deposition constant were in good agreement with field observations. The simulator was also able to predict the effects of a decreasing deposit thickness with increasing flow rates as observed in the Hassi Messaoud field. The paper further discusses a modified pseudo-transient simulator that is capable of incorporating the effect of deposit buildup on flow velocities and frictional pressure drop, which, in turn, affects the phase behavior of asphaltene. The differences between ADEPT and the pseudo-transient simulator is discussed. Simulation results show that incorporating the effect of deposit buildup causes a decrease in deposition rates with time, as reported from field observations.

INTRODUCTION

Asphaltenes are the heaviest and most polarizable fraction of a crude oil. They are defined as a solubility class in crude oil components that are are soluble in aromatic solvents, such as toluene or benzene, and insoluble in low-molecular-weight alkanes, such as *n*-heptane. Similar to waxes and inorganic scale, asphaltenes tend to cause arterial blockage of flow lines and other topside production facilities, such as separators and heat exchangers. Asphaltenes may also deposit in reservoirs. Asphaltenes are originally stable in crude oil at reservoir conditions. However, the phase stability of asphaltenes in oil is sensitive to the pressure and temperature conditions and oil composition changes potentially caused by the addition of light gases, solvents, and commingling with other oils or even changes because of contamination from other sources, such as oil-based drilling mud. When instability conditions are met, asphaltenes start phase separating from the oil and tend to deposit on walls of the wellbores and/or pipelines, which can cause significant production losses.[3] These problems therefore necessitate the ability to predict not only the possibility of asphaltene phase separation under various operating conditions but also its deposition tendencies. The phase stability of asphaltenes can be well-described by thermodynamic models, and this has been the subject of several publications. Application of cubic equations of state[3−5] and the statistical associating fluid theory (SAFT)-based equation of state[6−9] in modeling the stability of asphaltene in oil has been reported. However, the knowledge of possible asphaltene precipitation, although crucial, is only a part of the solution. It is equally important to predict the transport of these precipitated particles and identify their deposition tendencies. However, this line of research work has been hindered because of the complexity of asphaltene molecule structures and less understanding of their deposition mechanism.

There are a few studies published in the literature focusing on the prediction of asphaltene deposition in pipelines. The work by Ramirez et al.,[10] Jamialahmadi et al.,[11] Vargas et al.,[12] and Eskin et al.[13] describe the development of models to study asphaltene deposition. However, a review of the existing literature reveals that there is a lack of both qualitative and quantitative comparisons of the prediction of asphaltene deposition profiles with lab- and field-scale deposition profiles. Furthermore, the lack of complete field data substantially impairs the efforts of researchers in this area to be able to compare their new simulator predictions to field-observed situations. A recent publication[1] describes the development of a computationally efficient deposition simulator based on a transport model that accounts for the kinetics of asphaltene precipitation, aggregation, and deposition and discusses asphaltene deposition for two field cases reported in the literature. However, because of the lack of the experimental kinetic data measurements for the available field cases, the simulator had to be tuned to match the field-observed deposition profiles.

Received: April 27, 2012
Revised: July 24, 2012
Published: July 25, 2012

dx.doi.org/10.1021/ef300714p | *Energy Fuels* 2012, 26, 5702−5710

In this paper, the deposition simulator described in the earlier work has been used for the first time in a fully predictive manner to study the asphaltene deposition observed in one of the subsea pipelines in the Gulf of Mexico. All of the required kinetic constants, as described in the previous publication by Kurup et al.,[1] were directly measured from lab experiments. The methodology to extract the required model parameters is discussed. The paper also describes a methodology to scale up the deposition kinetic constant measured using the lab-scale capillary deposition experiment to predict deposition in the field conditions. Sensitivity analysis demonstrating decreasing deposition rates as a result of increasing flow rates, observed in many field cases, is also reported. The paper also describes the development of a pseudo-transient simulator that takes into account the effect of deposit build up on flow velocities and pressure profile, consequently affecting asphaltene phase behavior along the axial length.

DEPOSITION SIMULATOR STRUCTURE

Figure 1 shows the structure of the deposition simulator. A detailed description of the individual modules has been

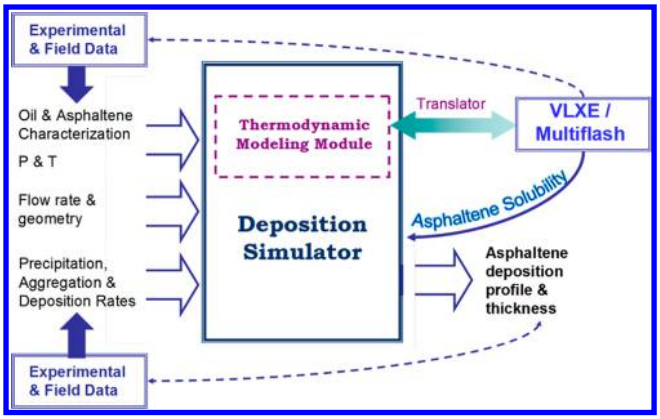

Figure 1. Deposition simulator structure.

provided in the previous publication by Kurup et al.[1] The detailed methodology of application of these individual modules has also been presented earlier.[18] Hence, only a brief description of the deposition simulator structure is provided. As seen from Figure 1, the deposition simulator consists of two modules: a thermodynamic module and a deposition module. When the deposition simulator has to be applied to study a particular field case, the first step in the application protocol is to thermodynamically model the live oil, which essentially constitutes the thermodynamic module of the deposition simulator. In this paper, the live oil is modeled using the perturbed-chain statistical associating fluid theory (PC-SAFT) equation of state.[6−9,14] The input parameters/measurements required for the development of the thermodynamic module are the live oil composition, density of stock tank oil/live oil, bubble points at different temperatures, and asphaltene onset pressures at different temperatures. With all of this information, the thermodynamic model of the oil can be built. The thermodynamic model gives insight into the envelope of precipitation and determines the stability of asphaltene at given pressure, temperature, and composition conditions. This solubility of asphaltene as a function of the pressure and temperature is a key input to the deposition module.

The deposition module consists of a mathematical model that describes the transport of precipitated primary asphaltene particles. The main components of the mathematical model are transport by advection and dispersion and the three kinetic processes: precipitation to form the primary particles, aggregation of these primary particles, and deposition of the primary particles onto the walls of the pipelines. In this paper, precipitation and deposition kinetics is modeled as a first-order process, while particle aggregation is modeled as a second-order process. The details of the mathematical model and the numerical methodology employed to solve the mathematical equations have been described in detail in the work by Kurup et al.[1] The input parameters required for the application of the deposition module are asphaltene solubility as a function of the pressure, temperature, and composition (input from the thermodynamic module), operating variables, such as length and diameter of the pipeline/wellbore, oil flow rate, and kinetic constants describing the kinetics of precipitation, aggregation, and deposition.

With these input parameters, the asphaltene deposition profile and thickness along the axial length of the wellbore/pipeline and the corresponding pressure drop can be predicted. The predictions can be benchmarked against both laboratory and field data, if available. The experimental strategies required to obtain the three kinetic parameters have been presented earlier.[18] In this paper, the precipitation and aggregation kinetic constants are extracted from laboratory asphaltene aggregation studies, while the deposition kinetic constant is obtained from the capillary deposition experiment.[15] It should be noted that the deposition rates measured through the capillary deposition experiments will help distinguish between the oils that have asphaltene precipitation problems but do not pose significant deposition issues and those that show severe deposition tendencies. Such oils may show high aggregation kinetics and low deposition kinetics.

DEPOSITION MODULE INPUT DATA ACQUISITION

Experimental Methodology. The application of the deposition module depends upon the acquisition of the kinetic constants of precipitation, aggregation, and deposition. The details of the capillary deposition apparatus used to determine the deposition kinetics have been published earlier[1,15−18] and, hence, will not be described in this paper.

In this work, the precipitation and aggregation kinetic constants are proposed to be extracted from the laboratory-scale asphaltene aggregation kinetic studies. For a given stock tank oil and a given *n*-alkane precipitant, a series of oil + *n*-alkane mixtures were prepared, each with the same oil/*n*-alkane volume ratio. The mixtures were aged in an oven at a given temperature. At different aging times, one of the mixtures was removed from the oven and filtered through a 0.22 μm filter paper to separate precipitated asphaltenes. The separated asphaltenes were thoroughly washed with *n*-alkane to remove any remaining oil, dried, and weighed to quantify the amount of aggregated asphaltenes that were separated at that particular aging time. Results from all of these separations yielded a kinetic aggregation curve for asphaltenes at that given oil/*n*-alkane ratio and temperature. Different *n*-alkanes, oil/*n*-alkane ratios, and temperatures may be employed to obtain different kinetic aggregation curves if needed. To ensure that asphaltene precipitation and aggregation would occur on all mixtures, an instant onset of asphaltene precipitation induced by that *n*-alkane was measured first and all of the oil + *n*-alkane mixtures were prepared with the *n*-alkane volume fraction exceeding that instant onset condition.

Mathematical Model for Aggregation. Asphaltenes are originally stable in crude oil at reservoir conditions; however, changes in the pressure and temperature conditions or the addition of

dx.doi.org/10.1021/ef300714p | Energy Fuels 2012, 26, 5702−5710

precipitating agents can trigger precipitation of asphaltene. The initial particles formed during this step are termed as primary particles. These primary particles then further aggregate with each other to form larger size particles. At every pressure, temperature, and composition condition, the thermodynamic equilibrium concentration of asphaltene determines the maximum concentration of asphaltene that can be stable in the oil without precipitating out. The concentration of asphaltene above this equilibrium concentration triggers precipitation of asphaltene.

The kinetic process of asphaltene precipitation and aggregation can be mathematically modeled, as shown below. As described earlier, the precipitation of asphaltene is modeled as a first-order kinetic process. The difference between the concentration of asphaltene in oil and the thermodynamic equilibrium concentration of asphaltene in oil at that pressure and temperature condition provides the driving force for asphaltene precipitation. The kinetics of aggregation is assumed as a second-order kinetic process, as used previously by other researchers in this area.[19] For simplicity sake, more detailed aggregation models reported by Professor Fogler's research group[20] have not been used in this study. The equations that describe the precipitation and aggregation of asphaltenes are

$$\frac{dC}{dt} = k_p(C_f - C_{eq}) - k_{ag}C^2 \quad (1)$$

$$\frac{dC_{ag}}{dt} = k_{ag}C^2 \quad (2)$$

$$\frac{dC_f}{dt} = -k_p(C_f - C_{eq}) \quad (3)$$

where C is the dimensionless concentration of the precipitated primary particle, C_{ag} is the dimensionless concentration of aggregated particles, C_f is the dimensionless concentration of asphaltene in the oil–precipitant mixture, and C_{eq} is the dimensionless thermodynamic equilibrium concentration of asphaltene. The initial concentration of asphaltene in the oil C_0 is used to non-dimensionalize all of the concentrations described in this work.

In this work, similar to the earlier publications,[1,12] it is assumed that only the primary particles participate in the deposition process. The large aggregated particles because of inertia are considered to be carried with the flow. Similar reasonable assumptions have been made in studies of other researchers in this area of modeling asphaltene deposition in pipelines.[13] The dimensionless particle relaxation time, given below, characterizes the time required by a particle to overcome its inertia and follow the fluid streamlines

$$\tau^+ = \frac{\rho_p {d_p}^2}{18\mu_f}\frac{u^{*2}\rho_f}{\mu_f} \quad (4)$$

where u^* is the friction velocity and can be calculated as $u^* = (\tau_w/\rho_f)^{1/2}$, where τ_w is the wall shear stress and can be calculated as $\tau_w = \rho_f f(U^2/8)$. The friction factor for a hydraulically smooth pipe is used, $f = 0.316/Re^{0.25}$.

Because the particle relaxation time depends upon the fluid velocity, calculations were performed for a range of fluid velocities and typical values of density and viscosity of live oil. It was seen that the particle size ranging from 0.2 to 2 μm defines the critical size of particles for varying fluid velocities. In this study, 0.2 μm is assumed as the critical particle size, viz., primary particle, and particles bigger than that are assumed to not participate in the deposition process.

Scaling of Deposition Kinetics. During normal production, generally, flow through wellbores/pipelines is turbulent. To investigate the scaling relationships between deposition in wellbores/pipelines and deposition in laboratory experiments, a review of various asphaltene deposition rates published in the literature was examined. Table 1 shows the asphaltene deposition rates published for field cases, such as Hassi Messaoud[2] and Kuwait Marrat[21] oil fields, and laboratory-measured deposition rates.[1,22] It can be seen that, in all of these cases, although the flow regimes are characterized from laminar ($Re < 1$) to turbulent ($Re > 100\,000$), the asphaltene

Table 1. Review of Asphaltene Deposition Rates

source	deposit thickness growth rate (cm/s)
Hassi Messaoud[2]	$\sim 2.0 \times 10^{-7}$
Marrat[21]	$\sim 2.5 \times 10^{-7}$
capillary deposition test[22]	$\sim 1.0 \times 10^{-7}$
capillary deposition test[1]	$\sim 1.0 \times 10^{-7}$

deposition rates are not very significantly different and are comparable within an order of magnitude. On the basis of this observation, in this work, we assume that the deposition process is not dominated by transport occurring in the core flow but dominated by transport and kinetics occurring in the laminar boundary layer adjacent to the wall of the wellbore/pipeline. Hence, in this work, the deposition kinetic constant is proposed to be obtained from the capillary deposition experiment. The laminar flow in the capillary experiment is assumed to represent the laminar boundary layer occurring in the turbulent wellbore/pipeline flows.

The mathematical model used in the deposition module was therefore modified to take into account the presence of the boundary layer, as shown in Figure 2. C is the concentration of asphaltene in the

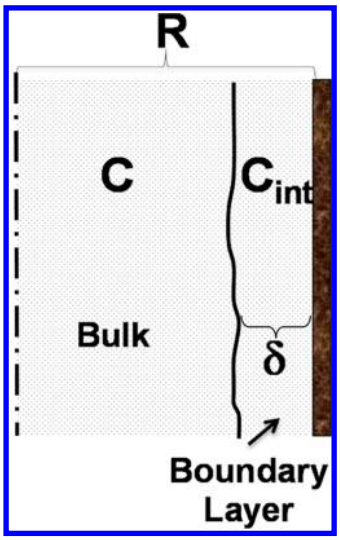

Figure 2. Laminar boundary layer near the wall.

bulk, while C_{int} is the concentration in the boundary layer of thickness δ. The mass balance for an axial segment δz can therefore be written as

$$V_{cell}\frac{\partial C}{\partial t'} = -V_{cell}U_z\frac{\partial C}{\partial z'} + V_{cell}D_{ax}\frac{\partial^2 C}{\partial z'^2} + V_{cell}k_p(C_f - C_{eq}) - V_{cell}k_{ag}C^2 - V_{int}R_{int} \quad (5)$$

where V_{cell} and V_{int} are the volumes of the axial segment and boundary layer segment, respectively. R_{int} is the rate of asphaltene depletion because of the deposition process. Rearrangement of the equations gives

$$\frac{\partial C}{\partial t} = -\frac{\partial C}{\partial Z} + \frac{1}{Pe}\frac{\partial^2 C}{\partial Z^2} + Da_p(C_f - C_{eq}) - Da_{ag}C^2 - \frac{V_{int}}{V_{cell}}\frac{L}{U_z}R_{int}$$

$$\frac{V_{int}}{V_{cell}} = \frac{2\pi R\delta\Delta Z}{\pi R^2\Delta Z} = \frac{2\delta}{R} \quad (6)$$

Two competing processes occur in the boundary layer near the wall: transport of asphaltene particles into the boundary layer because of the concentration difference between the bulk and the boundary layer and depletion of asphaltene because of deposition kinetics, and the rates of these processes can be written as

dx.doi.org/10.1021/ef300714p | Energy Fuels 2012, 26, 5702–5710

$$R_{\text{mass,tr}} = k_{\text{m}}\frac{\partial C}{\partial r} = k_{\text{m}}\frac{C - C_{\text{int}}}{\delta} = \frac{D_{\text{m}}}{\delta^2}(C - C_{\text{int}})$$

$$R_{\text{dep}} = k_{\text{d}}C_{\text{int}} \tag{7}$$

where k_{m} is the mass-transfer coefficient, D_{m} is the diffusion coefficient of the particle, and k_{d} is the deposition kinetic constant. At steady state, we have

$$R_{\text{int}} = R_{\text{mass.tr}} = R_{\text{dep}} = \frac{D_{\text{m}}}{\delta^2}(C - C_{\text{int}}) = k_{\text{d}}C_{\text{int}}$$

$$\phi C - \phi C_{\text{int}} = C_{\text{int}};\ \phi = \frac{D_{\text{m}}}{\delta^2}\frac{1}{k_{\text{d}}}$$

$$C_{\text{int}} = \frac{\phi}{\phi + 1}C \tag{8}$$

Equation 6 can be rewritten as

$$\frac{\partial C}{\partial t} = -\frac{\partial C}{\partial Z} + \frac{1}{Pe}\frac{\partial^2 C}{\partial Z^2} + Da_{\text{p}}(C_{\text{f}} - C_{\text{eq}}) - Da_{\text{ag}}C^2 - \frac{V_{\text{int}}}{V_{\text{cell}}}\frac{L}{U_z}k_{\text{d}}C_{\text{int}}$$

$$\frac{\partial C}{\partial t} = -\frac{\partial C}{\partial Z} + \frac{1}{Pe}\frac{\partial^2 C}{\partial Z^2} + Da_{\text{p}}(C_{\text{f}} - C_{\text{eq}}) - Da_{\text{ag}}C^2 - \frac{L}{U_z}k_{\text{d}}{}^*C \tag{9}$$

where

$$k_{\text{d}}{}^* = (k_{\text{d}})_{\text{cap}}\frac{2\delta}{R}\frac{\phi}{\phi + 1} = (k_{\text{d}})_{\text{cap}}ScF$$

$$ScF = \frac{2\delta}{R}\frac{\phi}{\phi + 1}$$

where ScF is a factor used to scale the deposition kinetic constant measured using capillary deposition experiments to predict asphaltene deposition in the wellbore/pipeline. A sensitivity analysis was performed to study the effect of parameters, such as particle size, Re, viscosity, and temperature, on the deposition scaling factor. A few important observations are shown in Figure 3. The scaling factor for three different values of the capillary deposition constant is shown for varying the particle size, varying Re, and two different viscosities of the oil. The thickness of the boundary layer was calculated using eq 12. In this case, mass transfer in the boundary layer was assumed to be the dominant mechanism. The diffusion coefficient was calculated using the Stokes–Einstein relation. From Figure 3, we can see that the scaling factor decreases with an increase in the particle size from 2 nm to 2 μm. From Figure 3, we can see that, as the value of the capillary deposition constant increases, the scaling factor is less sensitive to the parameters mentioned earlier. One of the most important observations that can be made from Figure 3 is that, as the Reynolds number (Re) increases, the scaling factor decreases, which means that, at higher flow rates, the scaled deposition constant and, consequently, the deposition rate decreases. This behavior has been observed in the field and has been reported in the publication by Haskett and Tartera.[2] The correlations used to calculate the boundary layer thickness, as explained later in this paper, show that, as Re increases, the boundary layer thickness decreases and, because the boundary layer thickness directly relates to the deposition scaling factor, an increase in Re causes a decrease in the deposit thickness. A comparison of the scaling factor at 0.1 cP viscosity against that calculated for 1 cP shows that the scaling factor decreases as the fluid viscosity increases. Thus, heavier oil with a higher viscosity would show lower deposition rates than oils with lower viscosity. Thus, the scaling factor and, hence, the scaled deposition constant are demonstrating most of the commonly seen field observations.

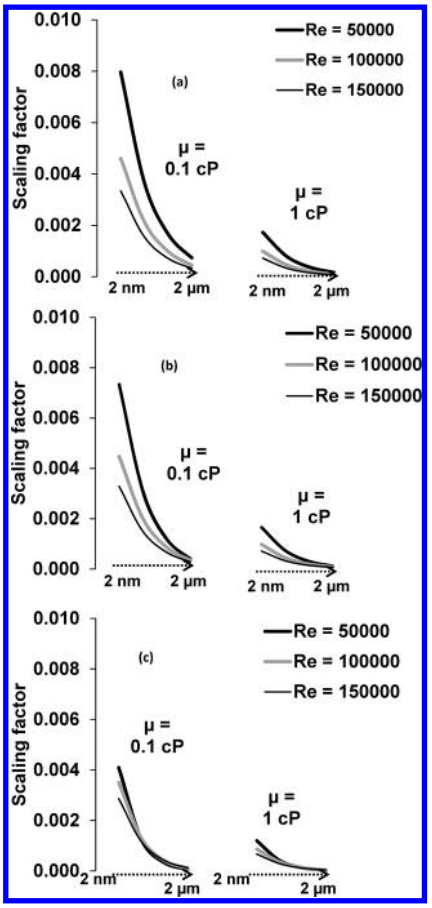

Figure 3. Sensitivity of the deposition scale-up factor. Deposition constant = (a) 0.0013, (b) 0.013, and (c) 0.13.

APPLICATION OF DEPOSITION SIMULATOR TO A FIELD CASE

The deposition simulator described in the earlier sections was then used to study asphaltene deposition in a subsea pipeline in the Gulf of Mexico. All of the input parameters required for the application of the thermodynamic and deposition modules were acquired, and the individual modules were developed.

Thermodynamic Module. The live oil was thermodynamically modeled using the PC-SAFT equation of state. The oil characterization and PC-SAFT parameter estimation methodologies reported in the work by Gonzalez et al.[7] and Panuganti et al.[9] have been followed. The live oil composition and density of stock tank oil were obtained from the operating company in charge of the production.[23] In this case, bubble point pressures for three different temperatures and the asphaltene onset pressure at one temperature were also provided. On the basis of these input data, the thermodynamic model was developed and the phase behavior of asphaltene as a function of the pressure and temperature is shown in Figure 4. The experimentally measured data points are also shown in this figure. The thin line represents PC-SAFT prediction of bubble points for different temperatures. The thick line represents PC-SAFT prediction of asphaltene upper onset pressures at different temperatures. The thick gray line is the lower onset pressure for different temperatures. Between the upper onset pressure curve and the lower onset pressure curve is the region in which asphaltene is unstable and represents the asphaltene precipitation envelope. Figure 4 also shows the pressure–temperature trace of the operating pipeline, which was obtained from the operating

dx.doi.org/10.1021/ef300714p | Energy Fuels 2012, 26, 5702–5710

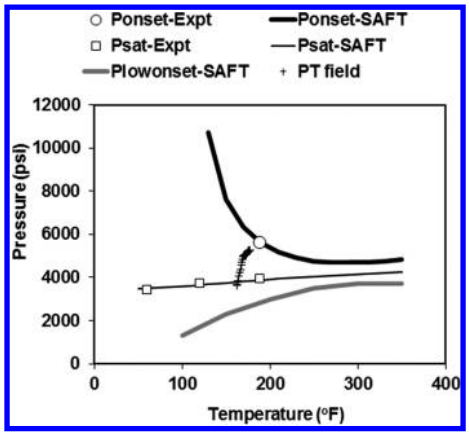

Figure 4. Asphaltene phase behavior.

company.[23] Because all of the operating points fall within the asphaltene precipitation envelope, the thermodynamic model predicts the possibility of asphaltene precipitation throughout the pipeline length. The thermodynamic model developed was then used to calculate the stability of asphaltene along the axial length of the pipeline as the pressure and temperature changes.

Deposition Module. The first step in the development of the deposition module is acquisition of the three kinetic constants, namely, the kinetics of precipitation, aggregation, and deposition.

Precipitation and Aggregation Kinetics. As described in the Experimental Methodology section, experiments were performed with the stock tank oil from this field with *n*-heptane (n-C_7) as the precipitant. Figure 5 shows the experimentally

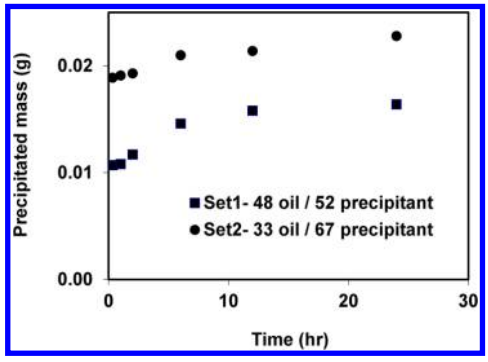

Figure 5. Experimental aggregation study.

measured weight percentage of asphaltene precipitated out of the oil/n-C_7 mixtures at different aging times for two different oil/n-C_7 mixing ratios. The mathematical model, as described in a previous section for the kinetics of precipitation and aggregation, was then used. The thermodynamic model was used to obtain the value of the thermodynamic equilibrium concentration for each case. The concentrations were nondimensionalized using the initial concentration of asphaltene in the oil, and the kinetic constants K_p and K_{ag} were then tuned to match the experimentally measured data points. The optimization solver in Microsoft Excel was used to ensure the best fit to the measured data points. Figure 6 shows the comparison of the simulation results to the experimentally measured data points. The best fit to the experimentally measured data points yielded is given in Table 2.

Deposition Kinetics. The capillary deposition experiment was employed to determine the asphaltene deposition rate. The

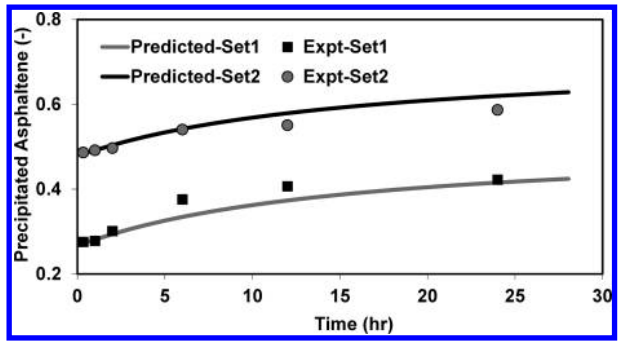

Figure 6. Extraction of precipitation and aggregation kinetic constants.

Table 2. Operating and Kinetic Parameters for the Subsea Pipeline

parameter	unit	quantity
pipe length	ft	52389
pipe diameter	in.	4.88
flow rate	barrels/day	29758
K_p	s^{-1}	1.32×10^{-3}
K_{ag}	s^{-1}	7.29×10^{-5}
K_d	s^{-1}	2.47×10^{-6}

experiment was conducted with chemical-free stock tank oil collected from that particular well. Propane was used as an asphaltene precipitant, and the deposition test was conducted at 70 °C, with a total flow rate of oil + propane at 12 cm^3/h. After the deposition test was completed, the *in situ* deposition profile and deposition flux were determined by the non-destructive glycerin injection method,[16,17] as shown in Figure 7 (data

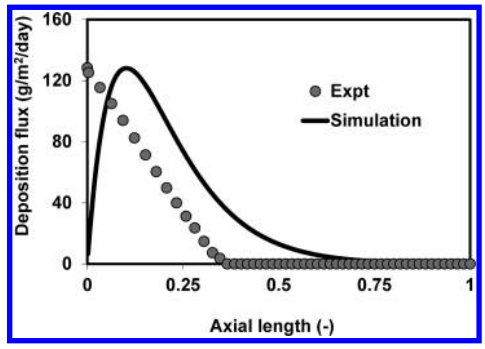

Figure 7. Determination of the deposition constant.

points). The axial dispersion mathematical model used to describe the precipitation and transport and deposition of asphaltene in a capillary tube was used to obtain the deposition kinetic constant. The mathematical model and the numerical solution methodology have been described in the work by Kurup et al.[1] A FORTRAN algorithm was used to solve the partial differential equations.

With all of these input parameters known, the deposition kinetic constant was tuned to match the model predictions to the experimentally determined deposition flux. Figure 7 shows the modeling results compared against the experimental measurements. It should be noted that the deposition constant was tuned to match the peak of the deposition flux because that determines the maximum constriction. The comparison between simulation and experimental results indicates that the simulation results show a delayed deposition compared to

dx.doi.org/10.1021/ef300714p | *Energy Fuels* 2012, 26, 5702−5710

experiments. This is due to the assumption used in solving the mathematical model that asphaltene precipitation begins only at the entrance of the pipe. This assumption means that there should be no delay between mixing of oil with the precipitant and entrance of this mixture into the pipe. Choosing a higher value of the deposition constant can decrease this discrepancy; however, this can cause a higher prediction of the deposition flux peak magnitude compared to experimental measurements. In reality, this delay cannot be fully eliminated, thereby leading to the discrepancy between the model prediction and the experimental measurement. Both lab-scale experimental measurement and model prediction show that the maximum deposition flux is close to the entrance of the pipe. This is due to the maximum concentration driving force for precipitation at the inlet. The driving force decreases along the length of the pipe as asphaltenes start precipitating out of the oil. The value of $(k_d)_{cap}$ obtained from this exercise is 1.4×10^{-3} s^{-1}.

Deposition Simulator Predictions. After the development of individual modules, the deposition simulator was then used to predict the location, magnitude, and growth rate of asphaltene deposition in the subsea pipeline under investigation. The thermodynamic equilibrium concentration as the temperature and pressure varies along the pipeline length is obtained from the thermodynamic model. Operating parameters, such as length and diameter of the pipeline and flow rate, were obtained from the operating company[23] and are summarized in Table 2. The three kinetic constants are also summarized in Table 2. The deposition kinetic constant is scaled as described previously using the scaling factor. Calculation of the scaling factor requires thickness of the boundary layer as an input. For a flow through a pipeline, three different layers are present near the wall. The outermost or thickest layer is the momentum boundary layer followed by a laminar sublayer and then the mass-transfer boundary layer. In this study, these three boundary layers are used in the calculation of the deposition scaling factor. The thickness of the momentum boundary layer can be calculated using the Prandtl boundary layer theory

$$\delta_{mom} = 62.7 D_t Re^{-7/8} \tag{10}$$

The laminar sublayer can be calculated as[13]

$$\delta_{lam} = 5\frac{\rho_f}{\mu_f u^*} \tag{11}$$

The mass-transfer boundary layer can be calculated as[24]

$$\delta_{mt} = \frac{D_t}{Sh} \quad \text{where } Sh = 0.023 Re^{0.8} Sc^{1/3} \tag{12}$$

Figure 8 shows the asphaltene deposition profile along the axial length of the pipeline using the three different scaling factors. Simulation is run for a deposition duration of 28 days. We can see that, although asphaltene precipitation probability is present along the entire length of the pipeline, the deposition profile peak occurs toward the exit of the pipe. This observation was confirmed by the field operators. The thermodynamic characterization of the live oil showed that the lowest solubility of asphaltenes in the oil occurred close to the bubble point, which occurs close to the end of the pipeline. The deposit thickness was calculated by considering that only 40% of deposit is asphaltene. This weight percent of asphaltene in the deposit was obtained from the thermodynamic calculation.

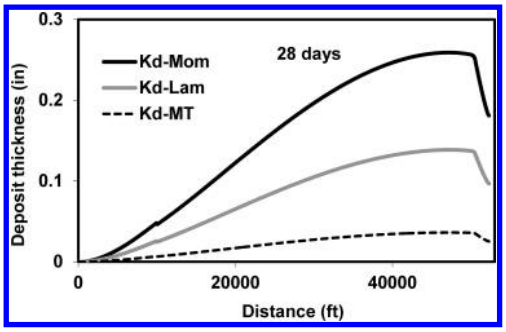

Figure 8. Deposition simulator predictions.

Saturates, aromatics, resins, and asphaltenes (SARA) analysis of the field deposit confirmed that the asphaltene content of the deposit is about 38%, verifying the accuracy of the thermodynamic model of the live oil.

Because this pipeline is a subsea pipeline, it was not possible to measure the deposit profile using a caliper, as reported in the literature for wellbore deposits of other fields.[2,21] However, pressure drop measurements were available for this subsea pipeline. During operation, it was observed that, as the production continued, an increase in the frictional pressure drop occurred, which was attributed to asphaltene deposition. For a production period of 28 days, a frictional pressure drop of 648 psi was observed by the field operator. Hence, with the deposition thickness profile predicted by the deposition simulator, the frictional pressure drop values were calculated for the three scaling factors and are reported in Table 3. The

Table 3. Frictional Pressure Drop Predictions[a]

	frictional pressure drop (psi)	
	smooth deposit	rough deposit
K_d based on	f = 0.013	f = 0.018
momentum boundary layer	502	700
laminar boundary layer	424	605
mass-transfer boundary layer	372	519

[a]Field-measured pressure drop = 648 psi.

field measured pressure drop is also reported in this table. The Darcy–Weisbach formula[25] was used to calculate the frictional pressure drop.

$$\Delta P_{friction} = f\frac{L}{D_t}\frac{U^2}{2g}\rho g \tag{13}$$

The frictional pressure drop is calculated by considering both a rough deposit and a smooth deposit. The Colebrook–White equation[25] was used to calculate the friction factor for a rough deposit. It can be clearly seen that the frictional pressure drop calculated from the deposition simulator thickness predictions are in the range of the field-measured pressure drops for deposition duration of 28 days. This is especially true when the deposit was considered rough and the laminar sublayer was considered as the boundary layer. This case demonstrates that the deposition simulator when coupled with the complete input parameters as described in this paper is able to make predictions comparable to field observations. This field case study is the first-time application of this simulator in a predictive manner. It should be noted that all of the input parameters were determined from the experiment, and none of the parameters used has been tuned to match the field

dx.doi.org/10.1021/ef300714p | Energy Fuels 2012, 26, 5702–5710

observation. However, for the application of this simulator to several other case studies demonstrated in this paper, parameter tuning was definitely required to gain further confidence in the use of this simulator for the design of asphaltene-related flow assurance risk assessment purposes.

Sensitivity Analyses. Simulations were performed to demonstrate the effect of the flow rate and, consequently, *Re* on the deposition scaling factor for this field case. Figure 9

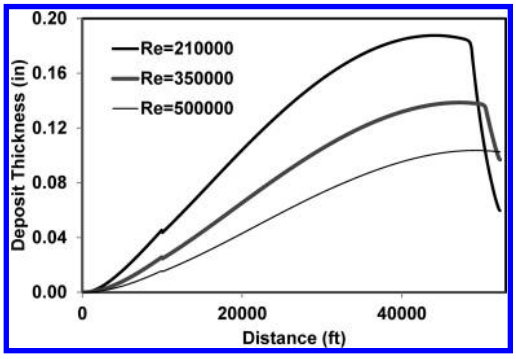

Figure 9. Effect of *Re* on the deposit thickness profile.

shows the effect of varying *Re* on the deposition profile. It can be seen that, as the oil flow rate increases, the deposit thickness for a given period decreases, similar to the observations made during the sensitivity analyses of the scaling factor. On the basis of the deposition profile, the total deposit mass was calculated. The mass was non-dimensionalized using the total mass of asphaltene flowing through the pipeline during the 28 day test period. Figure 10 shows the effect of *Re* on the percentage of

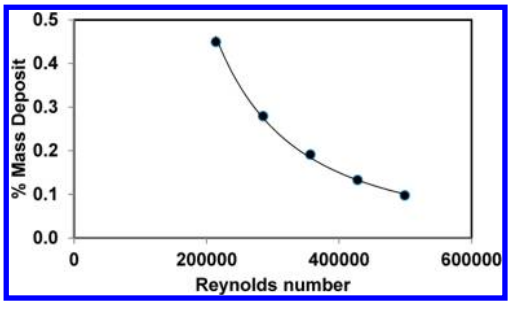

Figure 10. Effect of *Re* on the percent deposit mass with respect to total asphaltene flowing through the system.

dimensionless deposit mass. Figure 11 compares the percentage decrease in deposit mass against the percentage increase in flow rate/*Re*. It can be seen that doubling the flow rate or a 100%

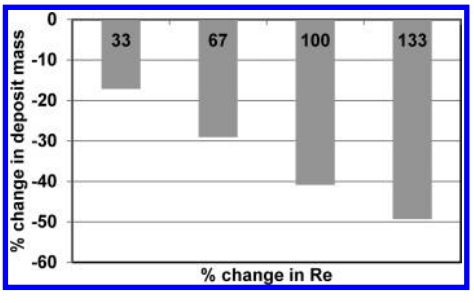

Figure 11. Percent increase in *Re* against percent decrease in deposit mass.

increase in the flow rate decreases the deposit mass by 41% in the total deposit mass. An increase in flow rate (*Re*) decreases the boundary layer thickness. As seen from the correlation of the deposition scaling factor, a decrease in the boundary layer thickness causes a decrease in the scaling factor and, consequently, decreases the deposit mass.

DEVELOPMENT OF A PSEUDO-TRANSIENT SIMULATOR

All of the simulation results described in the earlier sections were performed with a steady-state simulator that assumes a constant deposition rate with time. However, as deposit builds up, it restricts the available flow area, causing increased flow velocities. Increased constriction also increases the frictional pressure drop, changing the pressure profile along the axial length of the pipeline. The deposit buildup may also modify the temperature profile. A change in the pressure and temperature profile can alter the thermodynamic stability of asphaltene in oil as deposit builds up with time, which then affects the deposition rates. However, asphaltene deposition rates are generally very low, on the order of 10^{-7} cm/s (~1 mm/day) (cf. Table 1). Hence, the assumption of a constant deposition rate with time may still hold true. Nevertheless, it is important to check the differences in predictions obtained when a constant deposition rate is assumed against when the effect of the deposit is taken into consideration in the simulator. Hence, a pseudo-transient simulator was developed that incorporates the effect of the deposit on the transport rates and thermodynamic phase behavior. The pseudo-transient simulator recalculates the flow velocities based on a decreased pipe diameter at a preset time duration and also updates the pressure profile by considering the additional frictional pressure drop because of the deposit. The asphaltene solubility along the axial length is then recalculated at every time step based on the updated pressure profile, and then the new deposition rates are calculated. Currently, the effect of the deposit on the temperature profile is not very well understood, and hence, in this paper, the temperature effect has not been considered.

Figure 12 shows the comparison between the pseudo-transient simulator and the previously discussed steady-state

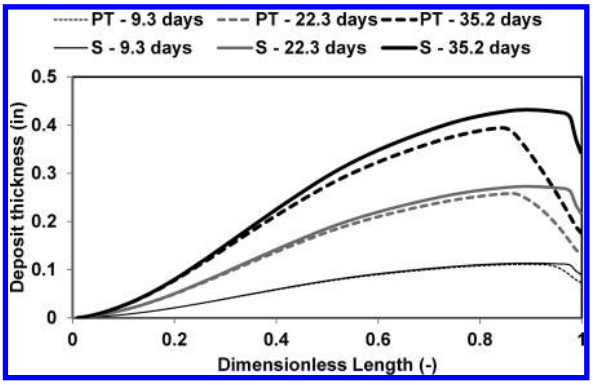

Figure 12. Pseudo-transient simulations (PT) against steady-state (S) simulations.

simulator for deposit buildup times of 9, 22, and 35 days. The solid lines are the pseudo-transient simulator results, while the dotted lines are the results obtained by assuming a constant deposition rate with time (steady-state simulator). It can be seen that, for a short duration, such as 9 days (deposit thickness

dx.doi.org/10.1021/ef300714p | *Energy Fuels* 2012, 26, 5702–5710

of ~0.1 in.), there is no difference between the magnitude of the deposit thickness predictions. For a period of 22 days (deposit thickness of ~0.25 in.), the difference between the magnitude is not significant, although the deposit profile is different. As the deposit builds up with time (for example, 35 days, with a 0.45 in. deposit), the difference between the two simulators becomes obvious in terms of both the deposit magnitude as well as the profile. It can be seen that, for 35 days, the pseudo-transient simulator predicts lesser deposit thickness compared to the steady-state simulator, which indicates that the deposition rate decreases with the buildup of the deposit. As the deposit constriction increases, the fluid velocity increases. Thus, the transport because of convection becomes too high compared to deposition rates, and the particles becomes carried away with flow. It is also seen that, as the deposit builds up, the maximum value of the asphaltene deposit thickness moves upstream of the flow toward the flow source. Figure 13 shows

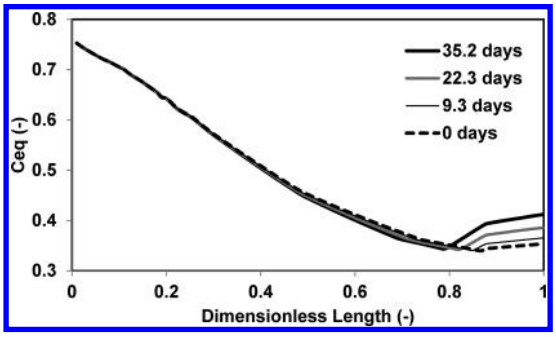

Figure 13. Variation of asphaltene solubility (C_{eq}) with deposit buildup.

the variation of asphaltene solubility (C_{eq}) along the axial length for the different durations of deposit buildup. It can be seen that, as the deposit buildup increases, the frictional pressure drop increases, which modifies the pressure profile, causing the asphaltene solubility curve to shift upstream of the flow. This causes the shifting of the deposit peak upstream of the pipeline.

It should be noted that the observation of a decrease in the deposition rate with an increase in the deposit buildup has been observed in the field, as reported by Haskett and Tarterra.[2] The movement of the deposit peak upstream of the wellbore/pipeline toward the bottom hole has also been reported in the literature.[2] Although these observations could also have been due to other effects, such as declining bottom hole pressure with continued production, it is still interesting to see that the simulator, at least for this field case, is able to predict these effects.

It should also be noted that, because of the iterative nature of the pseudo-transient simulator, it becomes very computationally expensive, especially as the duration of deposit buildup increases. Because for smaller deposit thickness, the difference between the steady-state and pseudo-transient simulators is not significant, for quick design estimates, the steady-state simulator can be used.

CONCLUSION

This paper shows the application of asphaltene deposition tool (ADEPT) to calculate the asphaltene deposition profile in a fully predictive manner for a subsea pipeline in the Gulf of Mexico for the first time. The required kinetic parameters were extracted from experimental data. The deposition constant obtained from the capillary deposition experiment was scaled up using the methodology described in this paper. With all of these input parameters, predictions of deposition profile and magnitude were made and compared to field observations. The location of the deposition peak was confirmed with field operators. Values of frictional pressure drops were calculated for the predicted deposition profile and compared to field measured pressure drop values. It was seen that there was good agreement between the predicted pressure drop and those measured at the field. The deposition simulator was thus able to give a good qualitative and quantitative estimate of asphaltene deposition. The scaled deposition constant has also been able to capture field observations, such as a decrease in deposit thickness for increasing flow rates.

In this paper, a pseudo-transient simulator was also developed that takes into account the effect of deposit buildup on flow velocities and pressure profiles affecting asphaltene phase behavior. It was observed that incorporation of these effects caused the deposition rate to decrease with an increase in deposit thickness. Increasing deposit thickness also modifies the deposition profile, making the deposition peak shift upstream of the flow. However, it was also observed that the difference between the predictions of the pseudo-transient simulator and ADEPT (which assumes a constant deposition rate with time) is not very significant for smaller deposit thicknesses, while the difference increases with an increasing deposit thickness. These differences will be enhanced for situations where the asphaltene deposition rates are high, while for situations with low deposition rates, ADEPT can give good estimates.

AUTHOR INFORMATION

Corresponding Author

*E-mail: mailtoanju@gmail.com.

Notes

The authors declare no competing financial interest.

ACKNOWLEDGMENTS

The authors thank Deepstar consortium for granting the approval to publish this paper. Anjushri S. Kurup and Walter G. Chapman acknowledge financial support from the Deepstar consortium.

NOMENCLATURE

C' = concentration of precipitated (phase-separated) asphaltene particles
C = dimensionless concentration of precipitated (phase-separated) asphaltene particles
C_0 = initial concentration of asphaltene solubilized in the oil phase
C_{eq} = dimensionless maximum concentration of asphaltene at equilibrium in the oil phase
C_f = dimensionless concentration of asphaltene solubilized in the oil phase
D_{ax} = axial dispersion coefficient
Da_{ag} = aggregation Damkohler number
Da_d = deposition Damkohler number
Da_p = precipitation Damkohler number
D_m = particle diffusivity
d_p = diameter of the particle
D_t = diameter of the pipe
f = friction factor

k_{ag} = aggregation kinetic constant
k_d = deposition kinetic constant
k_m = boundary layer mass-transfer rate
k_p = precipitation kinetic constant
L = axial length of the pipe/well bore
Pe = Peclet number
R = radius of the pipe/well bore
R_{dep} = deposition rate
Re = Reynolds number
R_{mass_tr} = rate of mass transfer
Sc = Schmidt number
ScF = scaling factor
Sh = Sherwood number
t = time
u^* = friction velocity
V_z = average axial velocity of the oil flowing through the pipe/well bore
z = axial length
Z = dimensionless axial length
$\overline{t}$ = residence time in a pipe
θ = dimensionless time
δ = boundary layer thickness
τ^+ = dimensionless relaxation time
ρ_f = density of the fluid
μ_f = viscosity of the fluid
ρ_p = density of the particle
$\Delta P_{friction}$ = frictional pressure drop

REFERENCES

(1) Kurup, A. S.; Vargas, F. M.; Creek, J. L.; Wang, J.; Buckley, J.; Subramani, H. J.; Chapman, W. G. *Energy Fuels* **2011**, *25* (10), 4506−4516.
(2) Haskett, C. E.; Tartera, M. *J. Pet. Technol.* **1965**, *17* (4), 387−391.
(3) Creek, J. L. *Energy Fuels* **2005**, *19*, 1212−1224.
(4) Burke, N. E.; Hobbs, R. E.; Kashou, S. F. *J. Pet. Technol.* **1990**, *42*, 1440−1446.
(5) Nghiem, L. X.; Coombe, D. A. *SPE J.* **1997**, *2*, 170−176.
(6) Ting, P. D.; Hirasaki, G. J; Chapman, W. G. *Pet. Sci. Technol.* **2003**, *21* (3 and 4), 647−661.
(7) Gonzalez, D. L.; Vargas, F. M.; Hirasaki, G. J.; Chapman, W. G. *Energy Fuels* **2008**, *22*, 757−762.
(8) Vargas, F. M.; Gonzalez, D. L.; Hirasaki, G. J.; Chapman, W. G. *Energy Fuels* **2009**, *23*, 1140−1146.
(9) Panuganti, S. R; Vargas, F. M.; Gonzalez, D. L.; Kurup, A. S.; Chapman, W. G. *Fuel* **2012**, *93*, 658−669.
(10) Ramirez-Jaramillo, E.; Lira-Galeana, C.; Manero, O. *Energ. Fuel* **2006**, *20* (3), 1184−1196.
(11) Jamialahmadi, M.; Soltani, B.; Müller-Steinhagen, H.; Rashtchian, D. *Int. J. Heat Mass Tran.* **2009**, *52* (19−20), 4624−4634.
(12) Vargas, F. M.; Creek, J. L.; Chapman, W. G. *Energy Fuels* **2010**, *24* (4), 2294−2299.
(13) Eskin, D.; Ratulowski, J.; Akbarzadeh, K.; Pan, S.; Lindvig, T. Modeling asphaltene deposition in oil transport pipelines. *Proceedings of the 7th International Conference on Multiphase Flow (ICMF)*; Tampa, FL, May 30−June 4th, 2010.
(14) Gross, J.; Sadowski, G. *Ind. Eng. Chem. Res.* **2001**, *40*, 1244−1260.
(15) Wang, J. X.; Buckley, J. S.; Creek, J. L. *J. Dispersion Sci. Technol.* **2004**, *25*, 287−298.
(16) Wang, J. X.; Buckley, J. S. *Estimate Thickness of Deposit Layer from Displacement Test*; Petroluem Recovery Research Center (PRRC), New Mexico Institute of Mining and Technology: Socorro, NM, June 2006 (revised Jan 2010); Technical Report PRRC 06-16.
(17) Wang, J. X.; Creek, J. L.; Fan, T.; Buckley, J. S. Asphaltene deposit distribution in capillary tests. *Proceedings of the 11th International Conference on Petroleum Phase Behavior and Fouling*; Jersey City, NJ, June 13−17, 2010.
(18) Kurup, A. S.; Buckley, J.; Wang, J.; Subramani, H. J.; Creek, J. L.; Chapman, W. G. *Proceedings of the Offshore Technology Conference*; Houston, TX, April 30−May 3, 2012; OTC 23347.
(19) Anisimov, M. A.; Yudin, I. K.; Nikitin, V.; Nikolaenko, G.; Chernoutsan, A.; Toulhoat, H.; Frot, D.; Briolant, Y. *J. Phys. Chem.* **1995**, *99*, 9576−9580.
(20) Maqbool, T.; Raha, S.; Hoepfner, M. P.; Fogler, H. S. *Energy Fuels* **2011**, *25* (4), 1585−1596.
(21) Kabir, C. S.; Hasan, A. R.; Lin, D.; Wang, X. An approach to mitigating wellbore solids deposition. *Proceedings of the Annual Technical Conference and Exhibition*; New Orleans, LA, Sept 30−Oct 3, 2001.
(22) Broseta, D.; Robin, M.; Savvidis, T.; Féjean, C. Detection of asphaltene deposition by capillary flow measurements; *Proceedings of the Society of Petroleum Engineers (SPE)/Department of Energy (DOE) Improved Oil Recovery Symposium*; Tulsa, OK, April 3−5, 2000; SPE 59294.
(23) Private communication with the operating company.
(24) Deen, W. M. *Analysis of Transport Processes*; Oxford University Press: New York, 1998.
(25) Whitaker, S. *Introduction to Fluid Mechanics*; Krieger Publishing Company: Malabar, FL, 1968.